Superconducting instability in the Holstein–Hubbard model: A numerical renormalization group study

C.–H. Pao
Department of Physics, National Chung Cheng University, Chia–Yi, 621 Taiwan, R.O.C.

H.–B. Schüttler
Center for Simulational Physics, Department of Physics & Astronomy, University of Georgia, Athens, GA 30602

(Auguest 25, 1997)

We have studied the d-wave pairing–instability in the two-dimensional Holstein-Hubbard model at the level of a full fluctuation exchange approximation which treats both Coulomb and electron-phonon (EP) interaction diagrammatically on an equal footing. A generalized numerical renormalization group technique has been developed to solve the resulting self-consistent field equations. The d-wave superconducting phase diagram shows an optimal T_c at electron concentration $\langle n\rangle \sim 0.9$ for the purely electronic Hubbard system. The EP interaction suppresses the d-wave T_c which drops to zero when the phonon-mediated on-site attraction U_p becomes comparable to the on-site Coulomb repulsion U. The isotope exponent α is negative in this model and small compared to the classical BCS value $\alpha_{BCS} = \frac{1}{2}$ or compared to typical observed values in non-optimally doped cuprate superconductors.

In recent years, growing experimental evidence has suggested that $YBa_2Cu_3O_7$ and, possibly, other cuprates are $d_{x^2-y^2}$–superconductors[1]. Anti–ferromagnetic (AF) spin fluctuation (SF) exchange has been proposed as a possible candidate mechanism for d–wave pairing. These AF spin fluctuation models are based on the notion that short-range, dynamical AF spin correlations, caused by the strong local Coulomb repulsion in the cuprates, may lead to a spatially extended pairing attraction.[1–4] Starting from purely electronic models, such as the Hubbard Hamiltonian, coupling to lattice vibrational degrees of freedom is usually neglected in this picture. However, except near certain "optimal" doping concentrations, many cuprates, including $YBa_2Cu_3O_7$, exhibit a quite noticeable doping dependent isotope effect[5]. This indicates that electron–phonon (EP) interactions could be important and should be included in the theory.

The goal of the present paper is to study the competition between phonons and AF spin fluctuation exchange by means of a self-consistent diagrammatic approach which explicitly includes phonon renormalizations to the AF spin fluctuations at the level of the effective interaction vertices. We formulate a full fluctuation exchange (FLEX)[2,3] approximation which treats Coulomb and EP contributions to the electron-electron interaction potential entirely on an equal footing. Our work goes substantially beyond previous treatments[6,7] which have included phonon effects only at the level of the one–particle self–energy.

Due to the retarded nature of the EP interaction, the problem is numerically not directly amenable to the recent fast Fourier transform (FFT)[8] or numerical renormalization group (NRG)[9] methods, developed for for the FLEX approximation to the pure Hubbard model. The present FLEX equations require certain large-scale fermion frequency matrix inversions which are numerically about 4 orders of magnitude more demanding than FLEX calculations with short-range instantaneous interactions. The numerical solution of this problem can be achieved only by means of a generalized, highly efficient matrix version of the original NRG method[9] which we have developed.

We start from the simplest microscopic Hamiltonian which includes both an on–site Hubbard U Coulomb repulsion and a local EP coupling to an Einstein phonon branch, the Holstein–Hubbard model[10],

$$H = -t \sum_{\langle ij\rangle\sigma} \Big[c^\dagger_{i\sigma} c_{j\sigma} + HC \Big] \; - \; \mu \sum_{i\sigma} n_{i\sigma} \; + \; U \sum_i n_{i\uparrow} n_{i\downarrow} + \sum_i \Big[\frac{\mathbf{p}_i{}^2}{2M} + \frac{1}{2} K \mathbf{u}_i{}^2 \Big] \; - \; C \sum_{i\sigma} \mathbf{u}_i \Big(n_{i\sigma} - \frac{1}{2} \Big) , \quad (1)$$

with a nearest neighbor hopping t, chemical potential μ, on–site Coulomb repulsion U, on–site EP coupling constant C, force constant K, and ionic oscillator mass M. The $c^\dagger_{i\sigma}$ ($c_{i\sigma}$) is the electron creation (annihilation) operator at site i and spin σ; $n_{i\sigma}$ is the number operator; and $\mathbf{u}_i$ is the local ionic displacement at lattice site i. The dispersionless bare phonon frequency is $\Omega_0 = (K/M)^{1/2}$ and the phonon-mediated on–site attraction is $U_p = C^2/K$.

Previous self-consistent field (SCF) studies[6] of the Holstein-Hubbard system have ignored the electron–electron exchange scattering which arises from the Pauli exclusion principle. The importance of this exchange vertex[2–4] can be most easily demonstrated in the limit of the negative-U Hubbard model with $U = -|U|$ and

$U_p = 0$. In this case, the direct interaction will give $2U$ (after summing over the electron spin index) and the exchange interaction contributes $-U$. The simplest mean field theory will then predict the CDW instability to occur at $|U|\bar{\chi}_{ph}(T) = 1$ (with exchange interaction) instead of $2|U|\bar{\chi}_{ph}(T) = 1$ (without exchange interaction). In the positive–U Hubbard model, the exchange interaction enhances the spin fluctuations and thus helps the d–wave instability while at the same time weakening the charge fluctuations. Also, high phonon frequencies or a flat electron band near the Fermi surface will tend to enhance the effect of the exchange vertex. To study particle–hole and particle-particle instabilities in this model, it is thus necessary to include both Coulomb and phonon contributions to the exchange vertex.

The bare interaction vertices for the FLEX equations shown in Fig.1, include the particle–hole [Fig. 1(b) and (c)] and the particle–particle [Fig. 1(d)] bare vertices, due to both the Hubbard U and the phonon propagator $v_p(i\nu_m) = -U_p\Omega_0^2/(\Omega_0^2 + \nu_m^2)$ [Fig. 1(a)] for boson Matsubara frequency $\nu_m = 2m\pi T$. The one–particle self–energy is then:[3,11]

$$\Sigma_k = \sum_{k'}\Big[V_2(\Delta k; i\omega_n) + V^{ph}(\Delta k; i\omega_n)\Big]G(k') + V^{pp}(\Delta k; i\omega_n)G^*(k') \ , \quad (2)$$

$$V_2(\Delta k; i\omega_n) = -v_p(\Delta\omega) + \sum_{i\omega_{n_1}}\Big[v_p(\Delta\omega) + U\Big] \Big[2v_p(\Delta\omega) - v_p(i\omega_n - i\omega_{n_1} - \Delta\omega) + U\Big]\bar{\chi}_{ph}(\Delta k; i\omega_{n_1}) \ , \quad (3)$$

$$V^{ph}(\Delta k; i\omega_n) = \sum_{i\omega_{n_1}} \frac{1}{2}\Big[D(1+D)^{-1} - D\Big]_{n,n_1}(\Delta k)\ v^D_{n_1,n}(\Delta\omega) + \frac{3}{2}\Big[M(1+M)^{-1} - M\Big]_{n,n_1}(\Delta k)\ v^M_{n_1,n}(\Delta\omega) \ , \quad (4)$$

$$V^{pp}(\Delta k; i\omega_n) = -\sum_{i\omega_{n_1}} \Big[S(1+S)^{-1} - S\Big]_{n,n_1}(\Delta k)\ v^S_{n_1,n}(\Delta\omega) + 3\Big[T(1+T)^{-1} - T\Big]_{n,n_1}(\Delta k)\ v^T_{n_1,n}(\Delta\omega) \ , \quad (5)$$

$$R_{n,n_1}(\Delta k) = v^R_{n,n_1}(\Delta\omega) \times \begin{cases} \bar{\chi}_{ph}(\Delta k; i\omega_{n_1}) \\ \bar{\chi}_{pp}(\Delta k; i\omega_{n_1}) \end{cases} \text{for } R = \begin{cases} D \text{ or } M \ , \\ S \text{ or } T \ , \end{cases} \quad (6)$$

where $k \equiv (\mathbf{k}, i\omega_n)$, $\Delta k \equiv (\mathbf{k} - \mathbf{k}', i\omega_n - i\omega_{n'})$, $\omega_n = (2n+1)\pi T$, the Green's function $G(k) = [i\omega_n - \epsilon_{\mathbf{k}} - \Sigma_k]^{-1}$, and the tight binding band $\epsilon_{\mathbf{k}} = -2t(\cos\mathbf{k}_x + \cos\mathbf{k}_y) - \mu$. The v^R_{n,n_1} are the bare vertices shown in Fig. 1(b-d). The bare particle–hole and particle–particle fluctuation functions are defined as:

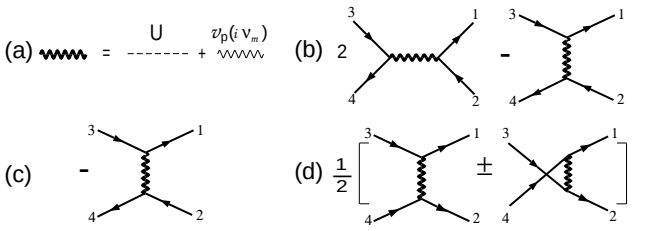

FIG. 1. The bare vertices of the Holstein–Hubbard model in the FLEX approximation. (a) The interactions of the on–site Coulomb U and Einstein phonon $v_p(i\nu_m)$. (b) Density vertex $v^D_{n_1,n_4}(i\nu_m) = [2v_p(i\nu_m) - v_p(i\omega_{n_1} - i\omega_{n_4}) + U]\ \delta_{n_1,n_2+m}\delta_{n_3+m,n_4}$. (c) Magnetic vertex $v^M_{n_1,n_4}(i\nu_m) = -[v_p(i\omega_{n_1} - i\omega_{n_4}) + U]\ \delta_{n_1,n_2+m}\delta_{n_3+m,n_4}$. (d) Singlet and triplet vertices $v^S_{n_1,n_4}(i\nu_m) = 1/2[v_p(i\omega_{n_1} - i\omega_{n_4}) + v_p(i\omega_{n_1} + i\omega_{n_4} - i\nu_m) + 2U]\ \delta_{n_1,-n_2+m}\delta_{-n_3+m,n_4}$, $v^T_{n_1,n_4}(i\nu_m) = 1/2[v_p(i\omega_{n_1} - i\omega_{n_4}) - v_p(i\omega_{n_1} + i\omega_{n_4} - i\nu_m)]\ \delta_{n_1,-n_2+m}\delta_{-n_3+m,n_4}$.

$$\bar{\chi}_{ph}(q; i\omega_n) = -\frac{1}{N}\sum_{\mathbf{k}} G(k+q)G(k) \ , \quad (7)$$

$$\bar{\chi}_{pp}(q; i\omega_n) = \frac{1}{N}\sum_{\mathbf{k}} G(k+q)G(-k) \ . \quad (8)$$

Because of the retarded nature of $v_p(i\nu_m)$, the bare vertices in Fig.1(b-d) depend explicitly on the internal frequency transfer and $i\omega_n$ can not be summed out here. The numerically most challenging part of the SCF calculation is thus the evaluation of the fluctuation potentials, V^{ph} and V^{pp}, because of the required fermion frequency matrix inversion in Eqs. (4,5). In a brute–force approach, this matrix dimension can become as large as 500×500 (the size of the entire fermion Matsubara frequency set) at T_c. Recent FFT and NRG techniques for the pure Hubbard FLEX equations are not directly applicable and we had to develop a generalized "fermion matrix" NRG method to handle the numerics efficiently[12].

Building upon the original NRG method[9], our generalized fermion matrix NRG employs a frequency–RG operation which separates the frequency space into high and low regions at each temperature in such a way that fermion frequency matrix dimensions will not increase as fast as T^{-1} when T is lowered. For a typical 8×8 matrix dimension, starting at some high temperature and large fermion frequency cut–off, we can keep the dimension below 30×30 after 6 factor-2 frequency–RG steps, corresponding to a temperature reduction from $4.0t$ to $0.0625t$. The fermion cut–off in the frequency RG steps changes from $100t$ ($\sim 12\times$ bandwidth) to $1.6t$ ($\sim 50\times T_c$). We then keep the same cut–off (without any further RG operation) and decrease the temperature slowly until the d–wave instability occurs[9]. A typical matrix dimension is then about 50×50 near the d–wave instability. The d–wave instability is determined by solving the eigenvalue problem for the singlet particle–particle kernel, constructed from the full interaction potential in Fig. 1(a),

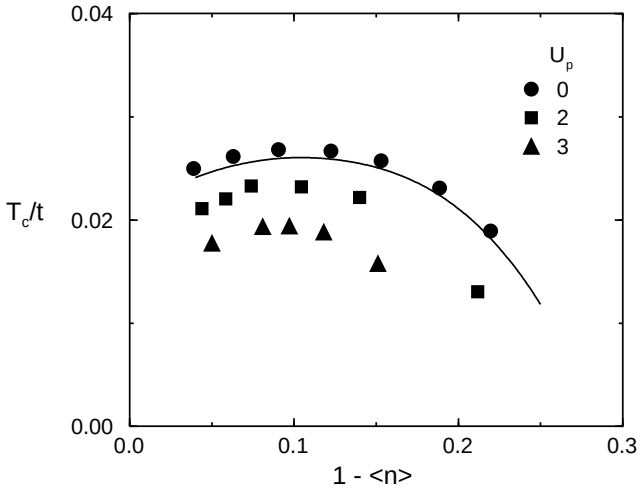

FIG. 2. Phase diagram of the d–wave instability with $U/t = 4$ and $\Omega_0/t = 0.5$ and different U_p on a 32^2 lattice. Solid line represents a Hubbard model calculation using the NRG method in Ref. [9] which does *not* involve the matrix inversion in Eqs. (4,5).

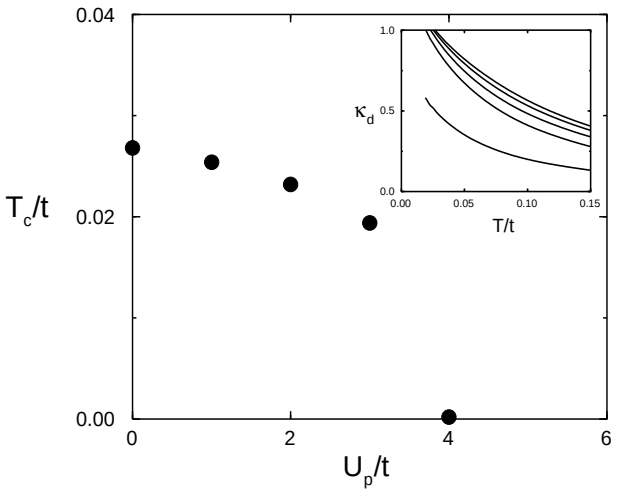

FIG. 3. d–wave T_c vs. EP potential U_p for $U/t = 4$, $\langle n\rangle = 0.9$, and $\Omega_0/t = 0.5$. Inset is the maximum d–wave eigenvalue vs. T for $U_p/t = 0, 1, 2, 3,$ and 4 (from top to bottom). T_c for $U_p/t = 4$ is extrapolated from the κ_d data at the lowest available T.

following Ref. 3. T_c is reached when the maximum paring eigenvalue $\kappa_d(T) = 1$. A 32×32 **k**-mesh covering the full 1st Brillouin zone has been employed in all of the calculations reported below.

Figure 2 shows the d–wave superconducting phase diagram of the Holstein–Hubbard model with intermediate Hubbard $U/t = 4$ for various EP coupling $U_p = 0$, 2, and 3 and an Einstein phonon frequency $\Omega_0/t = 0.5$. Increasing the electron concentration $\langle n\rangle$ towards half–filling ($\langle n\rangle \sim 1$) initially enhances the d–wave T_c until it reaches a maximum around $\langle n\rangle \sim 0.9$. Beyond that point, at hole doping $x = 1 - \langle n\rangle$ below $\sim 8\%$, the strong AF fluctuations actually reduce the d–wave T_c. This should be contrasted with early Hubbard model FLEX results in Ref. 2, where the detailed shape of the magnetic–superconducting boundary was not well determined and the d–wave T_c calculation was stopped when the magnetic eigenvalue exceeded unity. Here, we have used a finer lattice mesh and larger cut–off frequency and carefully pushed the d–wave calculations toward smaller hole doping.

In order to get a deeper understanding of the origin for the T_c maximum in Fig. 1, we have carried out a McMillan-type analysis[13] of the underlying pairing equations[3] by estimating the dimensionless Eliashberg parameter λ_d, which measures the pairing potential strength averaged over the Fermi surface in the d-wave channel, and $\lambda_Z = -\partial_\omega \mathrm{Re}\Sigma(k)|_{\omega=i0^+}$, which measures the strength of the quasi-particle mass enhancement, as well as the pair–breaking strength $\gamma = \left|\mathrm{Im}\Sigma(k)\right|_{\omega=i0^+}/T_c$, due to the quasi-particle damping. Expressed in terms of "renormalized" parameters[13] $\lambda_d^* = \lambda_d/(1+\lambda_Z)$ and $\gamma^* = \gamma/(1+\lambda_Z)$, our results show that both the pairing strength λ_d^* and the pair–breaking strength γ^* are monotonically increasing as $\langle n\rangle$ is pushed towards half–filling. Thus there are (at least) two competing effects at work here: While raising λ_d^* increases T_c, raising γ^* decreases it. Apparently, for overdoping, the doping variation of the pairing strength λ_d^* dominates T_c, making T_c initially rise with increasing $\langle n\rangle$. On the other hand, for underdoping, close to half–filling, the doping variation of the pair–breaking strength γ^* dominates and causes T_c to decrease with increasing $\langle n\rangle$. An additional, related effect is that the overall AF spin fluctuation energy scale softens as $\langle n\rangle$ approaches half-filling. This lowering of the relevant "boson" energy scale will also lower T_c.

The primary effect of EP coupling is to suppress the d–wave T_c, shown in Fig. 3 as a function of the EP potential strength U_p (from 0 to 4t) at fixed $U/t = 4$, electron filling $\langle n\rangle = 0.9$, and Einstein phonon frequency $\Omega_0/t = 0.5$. The corresponding maximum d–wave pairing eigenvalues κ_d as a function of temperature are plotted in the inset. Note that the d–wave T_c drops to "almost zero" (i.e. numerically inaccessible values) when U_p becomes comparable to U. This behavior is different from our earlier calculation[7] which ignored the phonon renormalization of the bare interaction vertices. In that case[7], T_c was suppressed only by the EP self-energy contribution, the suppression was much more gradual and T_c dropped only by about one half between $U_p = 0$ to $U_p \sim U$. Here, by contrast, the EP interaction directly counteracts the on-site Coulomb repulsion and thereby suppresses the AF spin fluctuation mediated pairing potential. The d–wave Eliashberg pairing strength λ_d and the pair–breaking strength γ are indeed found to be strongly suppressed by the EP interaction.

TABLE I. Isotope exponent α for $U/t = 4$ and $U_p/t = 2$.

Ω_0/t	0.125	0.25	0.5	1.0
$\langle n \rangle$				
0.96	-0.025	-0.059	-0.098	-0.166
0.90	-0.022	-0.053	-0.090	-0.127
0.87	-0.024	-0.061	-0.137	-0.196

An important feature of EP coupling is that it introduces an isotope effect into the electronic d–wave pairing mechanism. Table I shows results for the isotope exponent $\alpha = -d\log T_c/d\log M$ which becomes $\alpha = \frac{1}{2}d\log T_c/d\log\Omega_0$ in the present model, since the isotopic mass M enters only through Ω_0. In our previous studies[7] of the isotope effect, where the EP effect on the magnetic bare vertices was neglected, the isotope exponent α was quite small and negative for realistic phonon energies Ω_0. Here, as shown in Table I, we find qualitatively the same result, even though the EP effect on the AF spin fluctuations is now explicitly taken into account and suppresses T_c much more strongly. It is interesting to note that the absolute value of α has a minimum at the optimal doping concentration, a feature qualitatively reminiscent of the doping dependent isotope data in many cuprate systems.[5] However the observed overall magnitude of the effect in non-optimally doped cuprates, $|\alpha| \sim 0.5 - 1$,[5] is much larger than the present model predicts. This finding further supports the notion that the EP coupling in the cuprates could be effectively very much enhanced compared to conventional "strong-coupling" EP systems.[7]

In conclusion, we have studied the d–wave superconducting instability of the Holstein–Hubbard model in the FLEX approximation by means of a generalized, matrix version of the numerical renormalization group technique. Upon including both the particle–particle and particle–hole fluctuations, the d–wave T_c shows a maximum at electron filling $\langle n \rangle \sim 0.9$. The d–wave T_c is suppressed by increasing the EP potential U_p and tends to zero when $U_p \sim U$. Finally, the isotope exponents α are negative and small in magnitude, with typically $|\alpha| < 0.1$. While $|\alpha|$ exhibits a minimum at optimal doping concentration, the overall magnitude is far too small to explain observed isotope data in the cuprates. Our full FLEX results support the conclusions of earlier isotope calculations by the present authors.[7]

ACKNOWLEDGMENTS

We would like to thank Prof. N.E. Bickers for many helpful discussions. This work was supported by the National Science Council (Taiwan, R.O.C.) under Grant No. 862112-M194016T, by the National Science Foundation (U.S.A.) under Grant No. DMR-9215123 and by a Nat'l Chung Cheng University Young Faculty Research Grant. Computing support from UCNS (University of Georgia), the Pittsburgh Supercomputer Center, and the Nat'l Center for High–Performance Computing (NCHC, Taiwan, R.O.C.) are acknowledged.

[1] For an overview see: D.J. Scalapino, Physics Reports **250**, 329 (1995); B.G. Levi, Physics Today **46**, No.5, 17 (1993).
[2] N.E. Bickers, D.J. Scalapino and S.R. White, Phys. Rev. Lett. **62**, 961 (1989).
[3] N.E. Bickers and D.J. Scalapino, Ann. Phys. (N.Y.) **193**, 206 (1989); N.E. Bickers and S.R. White, Phys. Rev. B **43**, 8044 (1991).
[4] C.-H. Pao and N.E. Bickers, Phys. Rev. Lett. **72**, 1870 (1994); P. Monthoux and D.J. Scalapino, *ibid.*, 1874 (1994); 4176 (1994); T. Dahm and L. Tewordt, *ibid.* **74**, 793 (1995); S. Lenck, J.P. Carbotte, and R.C. Dynes, Phys. Rev. B **49**, 4176 (1994).
[5] M.K. Crawford *et al.*, Phys. Rev. B **41**, 282 (1990); Science **250**, 1390 (1990); (a) J.P. Franck *et al.*, Physica C **185-189**, 1379 (1991); Phys. Rev. Lett. **71**, 283 (1993); (b) J.P. Franck and D.D. Lawrie, *Proceedings of M^{2}S-HTSC-IV, Grenoble 1994*, Physica C (in press); for a recent review see: J.P. Franck, in *Physical Properties of High-T_c Superconductors IV*, ed. by D.M. Ginsberg (World Scientific, 1994), p. 189.
[6] F. Marsiglio, Physica C**160**, 305 (1989); Phys. Rev. B**42**, 2416 (1990); J. Low Temp. Phys., Vol. 87, 659 (1992).
[7] H.–B. Schüttler and C.–H. Pao, Phys. Rev. Lett. **75**, 4504 (1995).
[8] J.W. Serene and D.W. Hess, Phys. Rev. B **44**, 3391 (1991).
[9] C.–H. Pao and N.E. Bickers, Phys. Rev. B**49**, 1586 (1994), *ibid.* **51**, 16310 (1995).
[10] J. Zhong and H.–B. Schüttler, Phys. Rev. Lett. **69**, 1600 (1992); J.K. Freericks and M. Jarrell, *ibid.* **75**, 2570 (1995).
[11] The momentum and frequency summations are defined as: $\sum_k = \frac{1}{N}\sum_{\mathbf{k}} T \sum_n$ with N the total $\mathbf{k}$ points in 2D first Brillouin zone and T the temperature.
[12] C.-H. Pao and H.-B. Schüttler (unpublished).
[13] P.B. Allen and B. Mitrovic, in *Solid State Physics*, edited by H. Ehrenreich *et al.* (Academic, New York, 1982), Vol. 37, pp.1-97.